Light-Triggered Proton and Electron Transfer in Flavin Cofactors

Guifeng Li and Ksenija D. Glusac*

Department of Chemistry and Center for Photochemical Sciences, Bowling Green State University, Bowling Green, Ohio 43403

Received: December 13, 2007; Revised Manuscript Received: March 3, 2008

The pH dependent behavior of two flavin cofactors, flavin-adenine dinucleotide (FAD) and flavin mononucleotide (FMN), has been characterized using femtosecond transient absorption spectroscopy for the first time. The flavin excited state was characterized in three states of protonation (Fl^-, Fl, and FlH^+). We found that Fl and Fl^- exhibit the same excited state absorption but that the lifetime of Fl^- is much shorter than that of Fl. The transient absorption spectrum of FlH^+ is significantly different from Fl and Fl^-, suggesting that the electronic properties of the flavin chromophore become appreciably modified by protonation. We further studied the excited state protonation of the flavin and found that the protonation sites of the flavin in the ground and excited state are not equivalent. In the case of FAD, its excited state dynamics are controlled by the two conformations it adopts. At low and high pH, FAD adopts an "open" conformation and behaves the same as FMN. In a neutral pH range, FAD undergoes a fast excited state deactivation due to the "stacked" conformer. The transition from stacked to open conformer occurs at pH $\sim$ 3 (because of adenine protonation) and pH $\sim$ 10 (because of flavin deprotonation).

Introduction

Most living organisms rely on sunlight to successfully perform or regulate their function. Light is being used as a source of energy by plants (photosynthesis[1]), a source of information by animals (vision using rhodopsin photoreceptors[2]), and as a regulator of activity in both plants and animals (circadian rhythms using cryptochromes[3]). The enzymes that "process" light inputs always use one of the five cofactors: carotenoids, billins, chlorophylls, flavins, and pterins.[4] Flavins have attracted significant attention in the last years, because of the recent discovery of a large number of flavoprotein photoreceptors. The best-known light-triggered flavoprotein is DNA photolyase, which uses light to repair UV-induced pyrimidine dimer damages in DNA.[5] The cofactor in photolyase is a reduced deprotonated flavin-adenine dinucleotide ($FADH^-$) chromophore, and the enzymatic catalytic activity is achieved by a photoinduced electron transfer mechanism from photoexcited flavin to damaged DNA dimer. The second class of flavin-containing photoreceptors is the phototropin family,[6] which helps plants bend their organs toward light under weak light conditions (phototropism). Phototropins contain the flavin cofactor in its oxidized flavin mononucleotide (FMN) form, which undergoes a photochemical reaction that produces a conformational change in the phototropin, further triggering the phosphorylation of a kinase and initiating the signaling process. A third class of light-triggered flavoproteins is the BLUF protein family, which is found in photosynthetic microorganisms, such as cyanobacteria and flagellate algae.[7] Similar to phototropins in plants, BLUF proteins respond to light and trigger the movement of photosynthetic microorganisms in order to locate the optimal light conditions for photosynthesis. BLUF proteins contain a flavin cofactor in its flavin-adenine dinucleotide (FAD) form. The photomovement is initiated by a conformational change in the protein induced by a coupled proton and electron transfer between the FAD cofactor and the protein residues. The forth group of flavin containing photoreceptors are cryptochromes,[8] which are structurally very similar to DNA photolyases. Cryptochromes were recently discovered, first in plants as photoreceptors that regulate their circadian rhythms. This regulatory mechanism is believed to involve the protein conformational change induced by a photoinduced electron transfer. However, the exact mechanism of this light-triggered catalysis is yet to be determined. Cryptochromes were later found to regulate circadian rhythms in animals and humans as well. It is now well-established that cryptochromes in higher organisms have a "dark" function in the circadian rhythm, by acting as transcriptional repressors. However, it is still controversial whether their role in higher organisms is light-triggered.

To understand the mechanism of the above-mentioned photoreceptors, a large amount of research has been done on the excited state properties of FAD, FMN, and other flavin-based derivatives.[9–18] The lowest excited state of flavins is a state localized on the isoalloxazine moiety, according to evidence from absorption and fluorescence spectra, and the computational studies.[10] In the case of FAD, the lifetime of the π,π^* state can be dramatically quenched because of the complex formation between its isoalloxazine ring and its adenine moiety. The complex has been suggested many years ago by Weber,[9] who found that the fluorescence quantum yield decreases in FAD relative to FMN. Further spectroscopic evidence on complex formation has been obtained from fluorescence,[13,14] Raman,[15] transient UV/vis,[16] transient IR,[11] and NMR spectroscopy.[17] These studies suggest that FAD in solution exists in two conformations: an "open" form in which isoalloxazine and adenine rings are separated from each other, and a "stacked" conformation in which the two aromatic rings are in close proximity (Scheme 1). The "stacked" conformer is stabilized by the $\pi-\pi$ interactions between the aromatic rings and intramolecular hydrogen bonds along the phosphate−sugar backbone, as has been suggested by computational,[13] NMR,[17] and X-ray studies.[12] In a neutral aqueous solution, 80% of FAD is in the stacked conformation, while a change in the pH[19] or

* Corresponding author. E-mail: kglusac@bgsu.edu.

10.1021/jp7117218 CCC: $40.75
Published on Web 04/24/2008

SCHEME 1: (a) Structure of Flavin Adenine Dinucleotide (FAD) and (b) a Schematic Representation of the "Open" and "Stacked" Conformations Of FAD

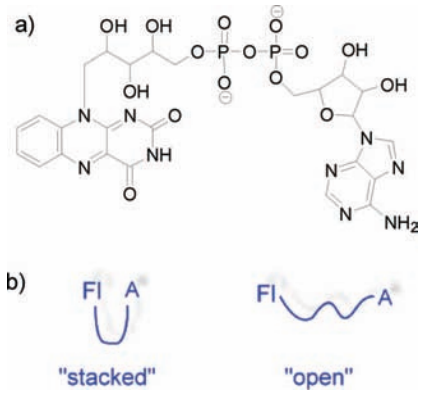

solvent polarity[16] can alter this ratio. The excited state lifetime of the "open" conformer is 2.6 ns, while the lifetime of the "stacked" form is only 10 ps.[14] This fast quenching of the flavin excited state is proposed to be due to the photoinduced intramolecular electron transfer from the isoalloxazine moiety to the adenine ring of FAD.[13] Even though energetics suggest an electron transfer mechanism, studies of the FAD singlet excited state have not led to the observation of transient radical species.[11,16] On the other hand, the production of a radical pair from the FAD triplet excited state has been detected by means of nanosecond transient absorption measurements in the presence of a magnetic field[20] and photochemically induced dynamic nuclear polarization (photo-CIDNP) experiments.[18]

Even though flavin derivatives have been extensively studied using traditional spectroscopic techniques, only a small number of reports use techniques with femtosecond time resolution. Such techniques can offer valuable information on the fast dynamics during the flavoprotein catalysis. To provide the ground work for these protein studies, we conducted a detailed study of flavin cofactors in aqueous solutions using optical femtosecond transient absorption spectroscopy. Specifically, this paper presents the pH dependence of the excited state dynamics of FMN and FAD. We report the transient absorption spectra of FMN in three states of protonation: FlH^+, Fl, and Fl^- (see Scheme 2). We further studied the excited state protonation of FMN, which occurs at pH $\sim$ 2. The results of this study are discussed in light of different ground and excited state acidity in FMN. In the case of FAD, the pH dependent behavior of FAD is more complex, because of the enrolment of the adenine moiety. While the same pH dependence due to the acidity of the isoalloxazine ring is present in FAD as well, there is an additional pH dependence that originates from the pH-induced conformational change between the "open" and the "stacked" form of FAD. A thorough analysis of this pH dependence is presented below.

Experiment

Sample Preparation. Flavin adenine dinucleotide disodium salt hydrate (FAD, HPLC grade) was purchased from Sigma, while flavin mononucleotide monosodium salt dihydrate (FMN, practical grade) was purchased from MP Biomedicals. Sodium hydroxide (NaOH, 97.4%, EMD), potassium phosphate (monobasic, KH_2PO_4, 99%, Aldrich Chemical Company, Inc.), and phosphoric acid (H_3PO_4, 85%, Lehigh Valley Chemical) were used to prepare phosphate buffer solutions. All of these chemicals were used as received. We prepared a series of FAD and FMN samples in 11 mM phosphate buffer solution with pH varying from -0.5 to 13. The 11 mM phosphate buffers in the pH range from -0.5 to 13 were prepared as follows: first, 0.748 g KH_2PO_4 was dissolved into 500 ml deionized water, then NaOH and H_3PO_4 were used to exactly adjust the pH value. The solution pH values were measured with an Oakton pH meter (pHTestr Basic). The FAD/FMN solutions in the buffer of appropriate pH were placed in a 2 mm quartz cell (Starna Cells, Inc). The FAD/FMN concentration was such that the absorption was in the 0.6–1.0 range at 400 nm. The absorption measurements were done using a UV$-$visible spectrophotometer (Varian Cary 50 Bio). Static luminescence spectra were collected by single-photon-counting spectrofluorimeter (FS 900, Edinburgh Analytical Instruments). The excitation was accomplished at 400 nm with a 450 W Xe lamp optically coupled to a monochromator (M300), and the emission was gathered at 90° and was passed through a second monochromator. The luminescence was measured with a Peltiercooled (-25.9°C), R955 red sensitive photomultiplier. The samples were put in quartz fluorometer cell (Starna Cell, Inc.) with 10 mm path length for fluorescence measurement. The concentration of FMN in different buffers was about 10–20 μM.

Transient Absorption Measurement. The laser system for the ultrafast transient absorption measurement was described previously.[21] Briefly, the 800 nm laser pulses were produced at a 1 kHz repetition rate by a mode-locked Ti:sapphire laser

SCHEME 2: Acid-Base Properties of FAD.

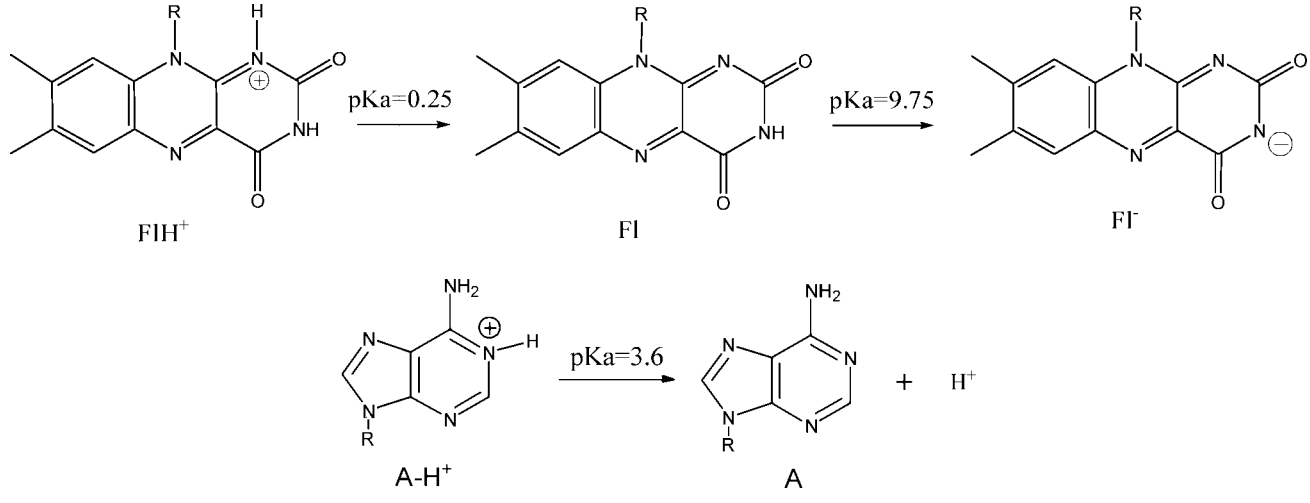

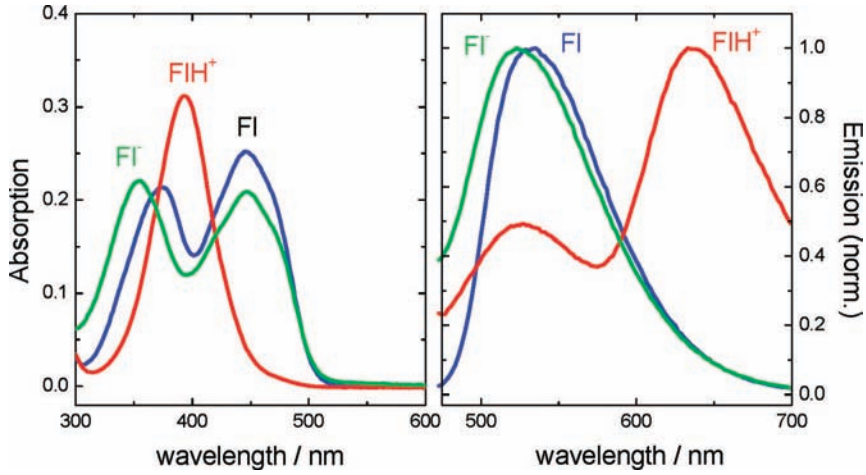

Figure 1. Absorption and emission spectra of FMN solutions at pH = −0.5 (FlH^+, red lines), pH = 7 (Fl, blue lines), and pH = 13 (Fl^-, green lines).

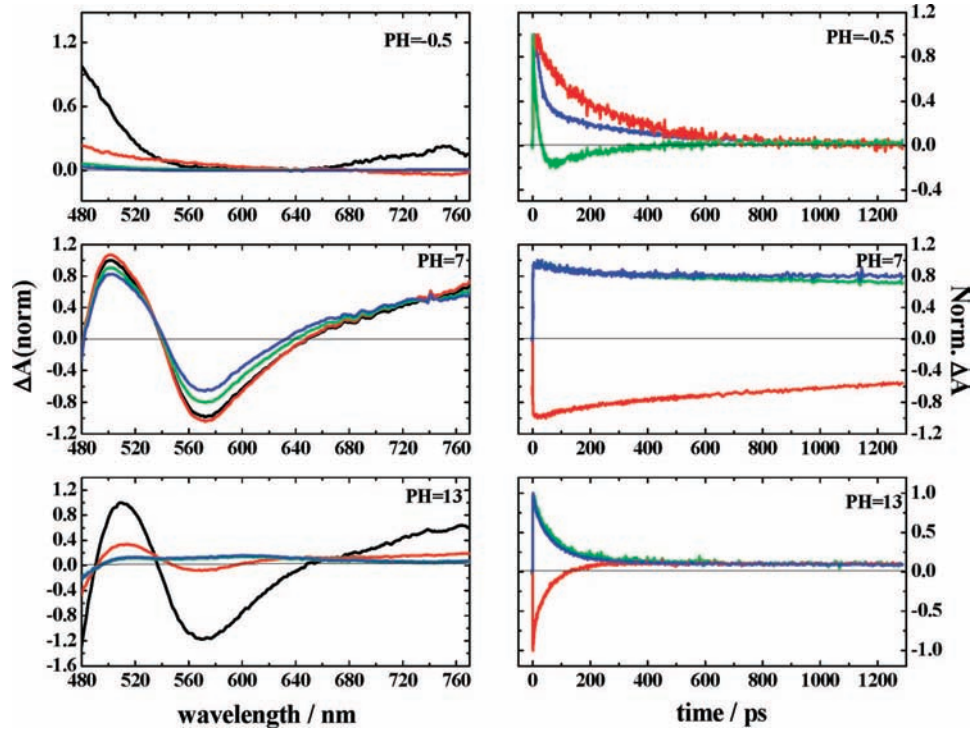

Figure 2. Transient absorption spectra (left panels) and decays (right panels) for FMN in aqueous solutions of different pH values: upper panels pH = −0.5; middle panels pH = 7; lower panels pH = 13. The transient absorption spectra are collected at time delays: 1 ps (black), 100 ps (red), 600 ps (green), and 1200 ps (blue). The time decays are collected at wavelengths: 510 nm (blue), 570 nm (red), and 750 nm (green).

(Hurricane, Spectra-Physics). The pulse width was determined to be fwhm = 110 fs using an autocorrelator (Positive Light). The output from a Hurricane was split into pump (85%) and probe (8%) beams. The pump beam (800 nm) was sent into a second harmonic generator (Super Tripler, CSK) to obtain a 400 nm excitation source. The energy of the pump beam was ~5 μJ/pulse. The probe beam (800 nm) was delayed by a delay stage (MM 4000, Newport) and then focused into a sapphire crystal for white light continuum generation between 450 and 900 nm. An optical chopper was used to modulate the excitation beam at 100 Hz frequency and obtain the value of the transient absorption signal. The relative polarization between the pump and the probe beams was set at the magic angle (54.7°). The pump and probe beams were overlapped in the sample. The flow cell (Spectrocell Inc., 0.7 ml volume with 2 mm pathlength), pumped by a Fluid Metering RHSY Lab pump (Scientific Support Inc.), was used to prevent photodegradation of the sample. After passing through the flow cell, the continuum was coupled into an optical fiber and input into a CCD spectrograph (Ocean Optics, S2000). The data acquisition was achieved using in-house LabVIEW (National Instruments) software routines.

The nanosecond measurement has been described previously.[22] Briefly, the excitation pulses of 7 ns with were produced as a third harmonic (355 nm) of a Q-switched Nd:YAG laser (Continuum Surelite I). The energy of the pump beam was about 3–4 mJ/pulse at the sample. The solutions were contained in 1 × 1 cm cells. The generated transient absorptions were monitored at right angles with respect to the laser beam. Kinetic data were obtained from computer averaging of at least 16 individual laser shots.

Data Processing. (i) Chirp correction: The group velocity dispersion of the probing pulse was determined using nonresonant optical Kerr effect (OKE) measurements.[23] The excitation

beam was focused on a sample cell containing carbon tetrachloride (Aldrich Chemical Company). The sample cell was placed in between a pair of crossed polarizers through which the probe beam was sent. The relative polarization between the incoming pump and the probe beams was set at 45°. The induced OKE signal was measured at various time delays. This measurement was used to perform a chirp correction in the collected transient absorption data by a code written with Matlab 7.1 software. First, the temporal evolution of the OKE signal at every wavelength was fitted to a Gaussian function. The value for the peak maximum obtained from the fit was used to construct the wavelength-dependent zero-times. Then, the time arrays from the transient absorption data were chirp-corrected by subtracting the value of zero-time at every wavelength. (ii) Noise reduction: The noise in the data was reduced using a singular value decomposition (SVD) method (Matlab 7.1). By using the SVD procedure, the data matrix $\Delta\mathbf{A}$ was decomposed into a product of three matrices according to equation:

$$A = USV^T$$

Matrix **S** is a diagonal matrix with the singular values as entries. Through visual inspection of the SVD components, we reconstructed a new matrix $\mathbf{S}_{NR}$ by keeping only the relevant singular values (usually the first 2–3 diagonal elements) and setting the rest of the diagonal elements to zero. Now, the noise-reduced data $\Delta\mathbf{A}_{NR}$ were reconstructed according to equation:

$$A_{NR} = US_{NR}V^T$$

The decays of the noise-reduced data $\Delta\mathbf{A}_{NR}$ were compared with the original data $\Delta\mathbf{A}$ at several wavelengths to ensure that the kinetic profiles were not altered.

Data Analysis. Transient absorption data were analyzed using SPECFIT/32™ Global Analysis System (Spectrum Software Associates, MA, USA). This program allows a decomposition of transient absorption data using kinetic models. The fitting process returns the predicted absorption spectra of individual colored species involved in the photochemical process along with their decay profiles. The analysis is achieved by a global analysis method that uses singular value decomposition method to reduce the size of the fitted data.[24]

Results and Discussion

FMN in the Protonated, Neutral and Deprotonated State. The acid−base behavior of FMN in aqueous solutions is due to two processes[25] presented in Scheme 2. The protonation of nitrogen in the position 1 of the isoalloxazine ring occurs at pH below 0.25. The second process involves a deprotonation of the nitrogen in position 3 and occurs at pH above 9.75. The absorption and fluorescence spectra of these species are presented in Figure 1. In order to characterize the excited state dynamics of the FMN in the protonated (FlH^+), neutral (Fl), and deprotonated (Fl^-) states, we collected the transient absorption spectra of FMN solutions at pH values of −0.5, 7, and 13. The results of these measurements are discussed in this section. While FAD behaves the same as FMN in the acidic and basic regions, it exhibits different behavior in the neutral state. This behavior will be discussed in the following sections.

The transient absorption spectra and time decays of FMN at pH = 7 (Fl) are presented in the middle panels of Figure 2. The spectrum of FMN at the early time $t = 1$ ps consists of a negative signal in the 540–670 nm range that is assigned to the stimulated emission of the singlet excited (^1Fl) state localized on the isoalloxasine ring. The rest of the optical range (480–540 nm and 670–760 nm regions) is covered by a positive signal

SCHEME 3: Kinetic Models Used to Fit the Excited State Dynamics of Flavins in Different States of Protonation

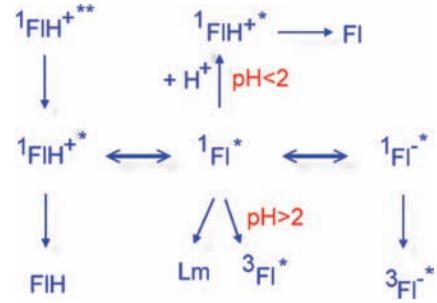

SCHEME 4: Photoreduction of FMN to Lumichrome

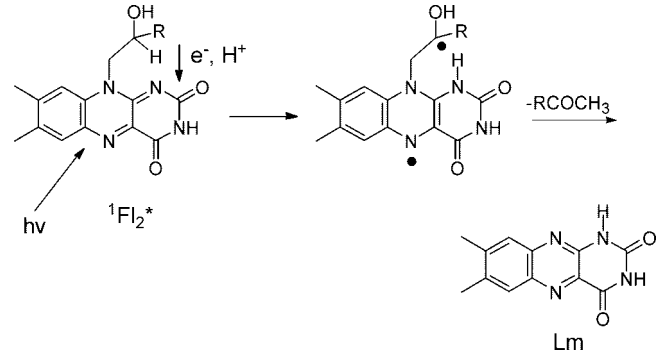

that is assigned to the absorption of the same ^1Fl state.[16] The absorption signal continues to evolve during the first 3 ps. This is why the spectrum collected at 100 ps delay is more intense than the one collected 1 ps after the excitation pulse. We believe this behavior to be due to internal conversion from higher excited states of the flavin. It is interesting to note that our result suggests a somewhat slower rate of internal conversion than the one reported previously (~250 fs).[16] This discrepancy might be due to the presence of phosphate ions used as a buffer in our FMN solutions, which might reduce the rate of thermal deactivation of the S_2 excited state. The effect of buffer molecules on the excited state behavior of flavins has been previously observed in the photoreduction studies of FAD and other flavins in aqueous solutions.[26] While the origins of this buffer effect are not known, it was shown that the reduction occurs with twice the efficiency when the buffer is present in solution. Once the ^1Fl state has fully developed, it decays within several nanoseconds to produce a new transient. This new absorption band can be observed in the spectrum recorded 1.2 ns after the excitation pulse, which exhibits a slightly different shape from the transient spectrum obtained at the initial time delays. Specifically, a new absorption band is observed in the 600–700 nm range. The dynamics of this process can be observed in the middle right panel of Figure 2, which shows that selected wavelengths exhibit different decay dynamics. At a time delay of 1.2 ns, the signal at 570 nm decays to 60 % of its initial intensity, while the decays at 510 nm and 750 nm decay only to ~80 % of its initial intensity.

We analyzed the data using a model according to which the FMN singlet excited state undergoes intersystem crossing to produce an FMN triplet excited state and found the rate of this process to be $k_{ISC} = 2 \times 10^8\ s^{-1}$ (Scheme 3). However, the fitting results suggest that an additional deactivation pathway to the ground state occurs from the initial FMN singlet excited state. The rate of this process is $5.4 \times 10^9\ s^{-1}$, and it probably originates from the fraction of FMN conformers that contain a

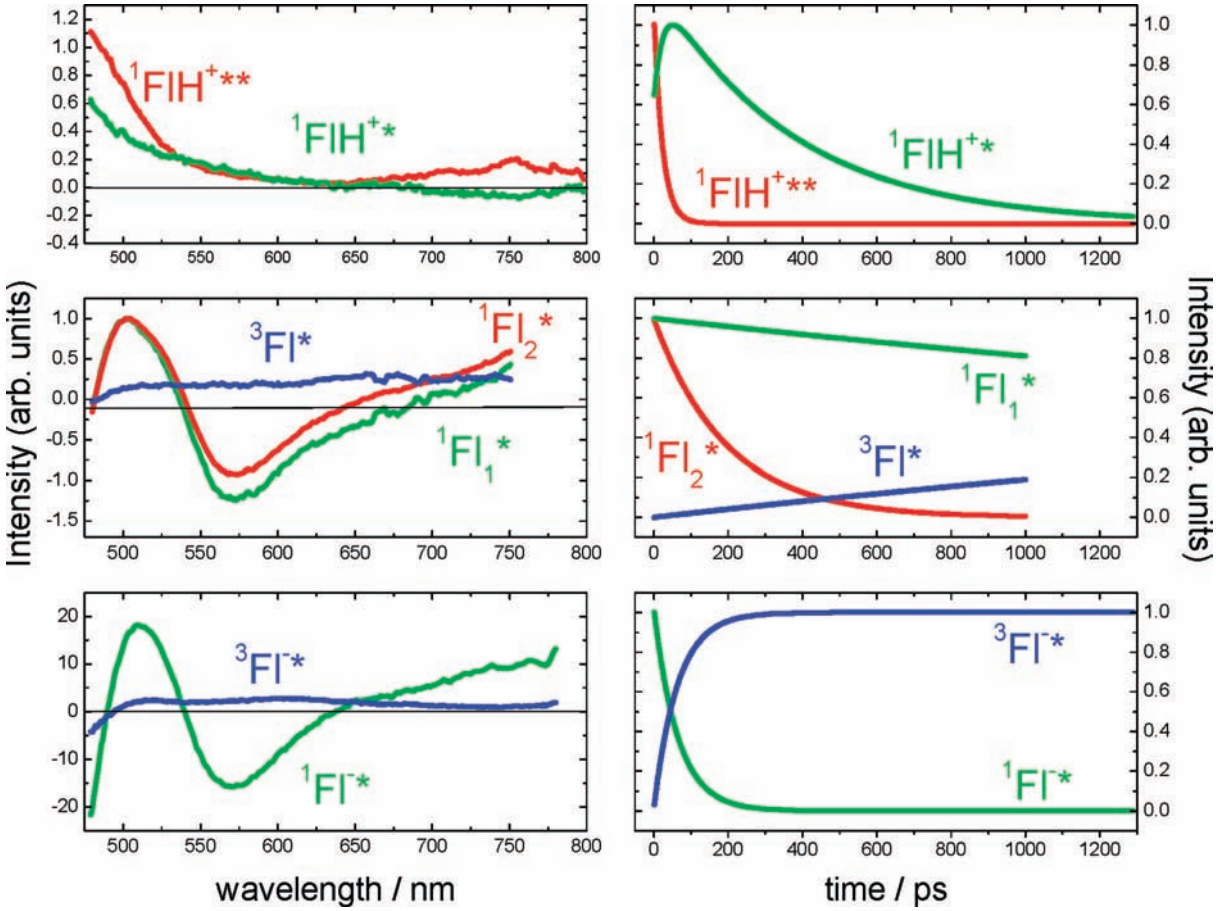

Figure 3. The absorption spectra and time decays of the transient components involved in the excited state dynamics of FMN at pH = −0.5, 7, and 13. The curves were obtained by fitting the experimental data to models described in Scheme 3.

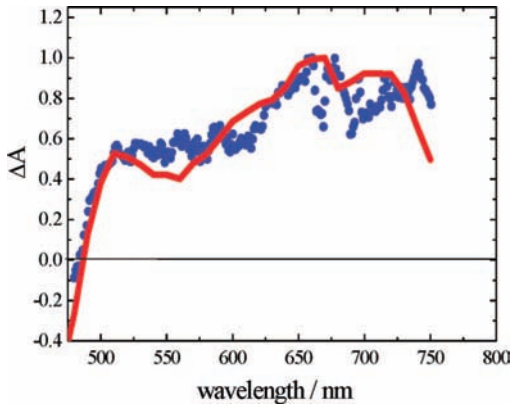

Figure 4. Comparison of the FMN triplet excited state ($^3Fl^*$) spectrum obtained from a nanosecond transient absorption experiment (red line) and the one obtained by analyzing the femtosecond transient absorption spectrum (scattered plot).

sugar backbone in close proximity to the isoalloxazine ring ($^1Fl_2$). For those conformers, there is a possibility for proton-coupled electron transfer from sugar backbone to the isoalloxazine ring (Scheme 4). It is well-documented in the literature that this process occurs in the triplet excited state and that it leads to photoreduction of FMN to lumichrome.[27,28] We think that this reaction occurs via a singlet excited state as well, which is supported by the previous experiments involving fluorescence quenching of various flavins.[26] We did not observe the production of lumichrome, since it absorbs out of the spectral window of our transient absorption measurements. We are currently expanding our investigation to the transient mid-IR measurements in order to investigate this fast FMN decay in more detail. The spectra and decays of the transient involved are presented in the middle panels of Figure 3. We compared the spectrum of the FMN triplet excited state obtained from the fit with the spectrum of FMN triplet excited state obtained using nanosecond transient absorption setup (Figure 4). The agreement between these two spectra and the spectrum reported in the literature[29] is very good, thus providing a confirmation that our fitting model is correct.

The transient absorption spectra and decays of FMN at pH = 13 (Fl^-) are presented in the lower panels of Figure 2. The spectrum of $^1Fl^-$ obtained 1 ps after the excitation pulse exhibits the same characteristics as the spectrum of ^1Fl obtained in the neutral pH range. However, the $^1Fl^-$ exhibits a much shorter lifetime (~50 ps), as can be seen from the decay curves at 500, 570, and 750 nm. In addition, a new absorption band appears which can be observed as a positive signal in the 570 nm decay curve. Since this transient exhibits a long lifetime (we do not observe any decay on the timescale of our measurement, 1.2 ns), it probably originates from the triplet excited state $^3Fl^-$. We fit the data to the model presented in Scheme 3 and found the rate of intersystem crossing (ISC) to be 1.56×10^{10} s^{-1}, which is much higher than the rate observed for ^1Fl. The higher rates of $^1Fl^-$ deactivation could arise because of the role of the $^3n,\pi^*$ (^2T) state in the $^1S-^1T$ (π,π^*) ISC process. Theoretical calculations of the ISC process in neutral flavins suggest that ISC occurs via $^3n,\pi^*$ as an intermediate.[30] While the calculations have not been performed on deprotonated flavins, it is possible that the energy of the $^3n,\pi^*$ state in these molecules is lowered because of the deprotonation. This would lead to an even

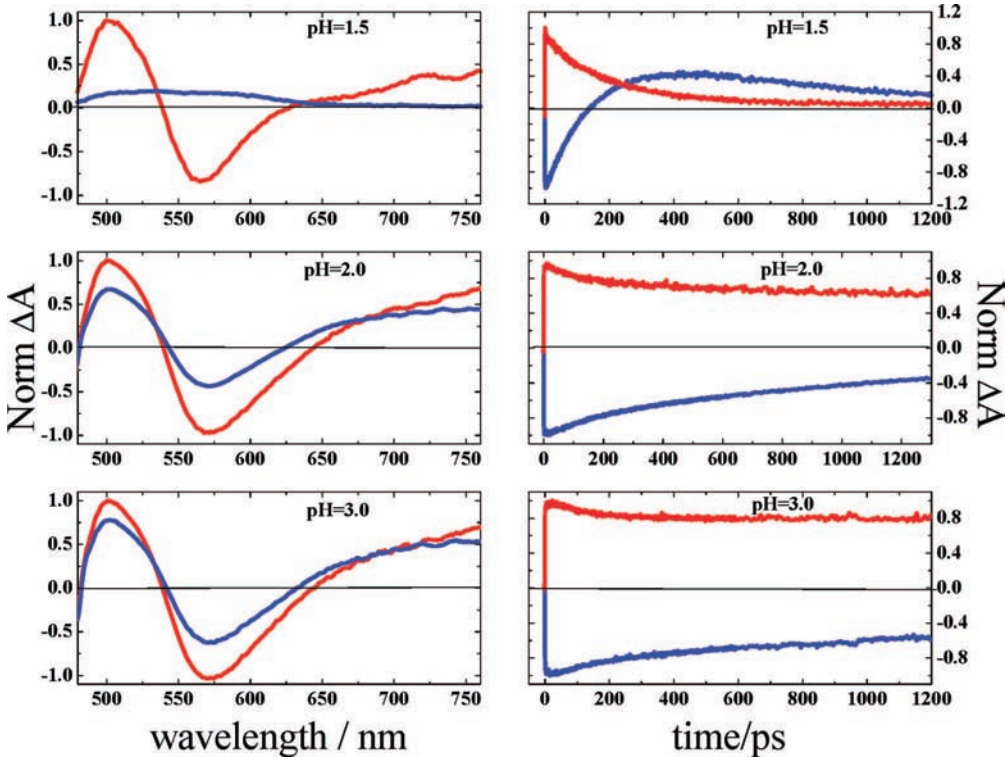

Figure 5. The transient absorption spectra (left panes) and decays (right panels) for FMN at pH = 1.5 (upper panels), pH = 2 (middle panels), and pH = 3 (lower panels). The spectra were collected at time delays of $t = 6$ ps (red line) and $t = 1000$ ps (blue line). The decays were obtained at $\lambda = 575$ nm (blue line) and $\lambda = 750$ nm (red line).

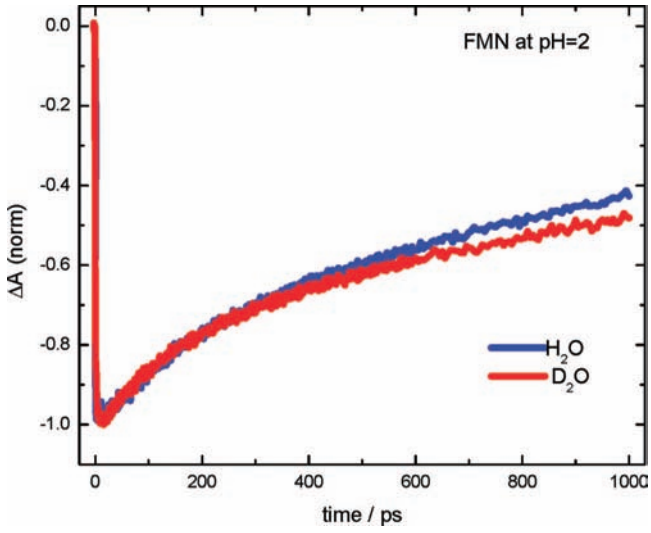

Figure 6. The excited state dynamics of FMN at pH = 2 in H_2O (blue) and D_2O (red).

stronger involvement of this state in the S−T ISC process and a faster deactivation of the ^{1}S state. The spectra and decays of $^1Fl^-$ and $^3Fl^-$ are presented in the lower panels of Figure 3.

The transient absorption spectra and decays for the protonated FMN (FlH^+) are presented in the upper panels of Figure 2. The spectrum obtained 1 ps after the excitation pulse looks very different from the ones obtained for Fl^- and Fl. The full spectral window is covered by a positive signal with $\lambda_{max} = 480$ nm. This transient decays within ~20 ps to produce new species with absorption in the blue portion of the spectral window and stimulated emission in the red region (above 700 nm). This behavior is best observed in the decay curve at 750 nm (upper right panel of Figure 2). The positive signal at $t = 0$ rapidly decays, and the negative-going signal is observed with a maximum build-up after ~100 ps. The subsequent decay of the stimulated emission signal occurs within several hundreds of picoseconds. This low-energy stimulated emission signal is consistent with the fluorescence spectra of FlH^+ presented in Figure 1. We assign the second transient to the FlH^+ lowest singlet excited state because of the fact that it exhibits stimulated emission. The stimulated emission occurs at low energy with the lifetime of $^1FlH^{+}$* of only ~200 ps. This is probably due to the small HOMO-LUMO bandgap in FlH^+, which leads to a fast thermal deactivation from the first excited state to the ground state dictated by the energy gap law.[31] The initial transient observed at early times must then originate from higher excited states ($^1FlH^{+}$**) which deactivate and populate the FlH^{+}* within ~20 ps. This deactivation of $^1FlH^{+}$** is much slower than the one expected for the internal conversion process (~1 ps), especially in the case of a large molecule such as FMN. We assume that a large activation barrier exists between the two excited states involved in the process. The spectrum of the $^1FlH^{+}$** probably belongs to the ^{1}n,π* (^{2}S) state of FMN.[30] The slow internal conversion from $^1FlH^{+}$** to $^1FlH^{+}$* suggests that these two levels are energetically close to each other.

In summary, the spectra and decays of the lowest singlet excited states of FlH^+, Fl, and Fl^- are presented by solid lines in Figure 3. The spectra of ^{1}Fl* and $^1Fl^-$* are almost identical, but the rate of intersystem crossing in $^1Fl^-$* is much higher than that of the ^{1}Fl* state. In contrary, $^1FlH^{+}$* exhibits significantly different spectral features. These results suggest that the deprotonation of nitrogen in the position 3 does not significantly disrupt the electronic distribution of the absorbing moiety, while the protonation of the nitrogen in position 1 strongly modifies the chromophore.

Excited State Protonation. In the pH = 1–3 region, both FMN and FAD show a large change in their excited state dynamics. We will present only the results obtained for FMN

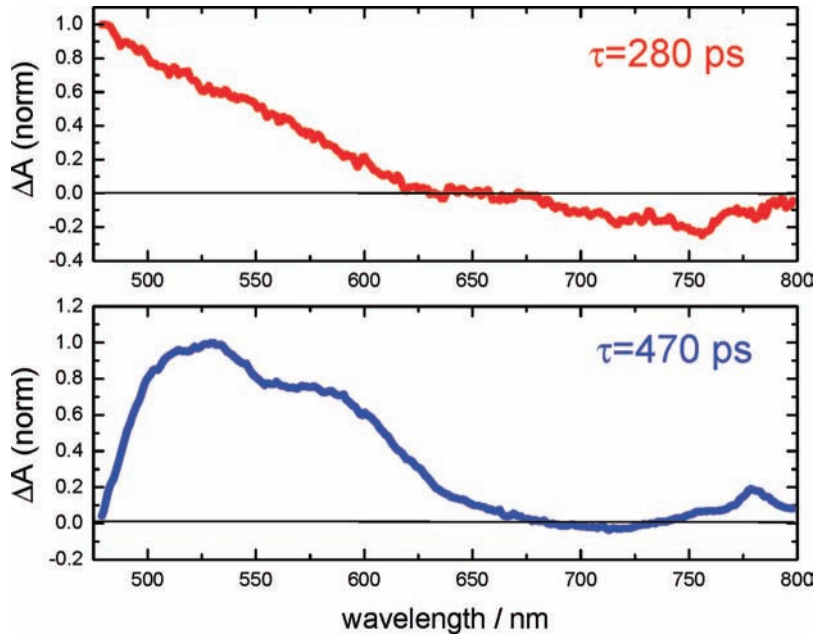

Figure 7. The comparison of FlH^+ transient absorption spectra obtained by fitting the experimental data obtained for FMN at pH = −0.5 (upper panel) and pH = 1.5 (lower panel).

solutions, since the same dynamics were observed for FAD solutions. Figure 5 shows the data obtained at pH = 1.5, 2, and 3. At pH = 3, FMN decay dynamics are the same as the ones observed at pH = 7 (see Fl in the previous section). The spectrum consists of stimulated emission and excited state absorption features that exhibit lifetime on the order of several nanoseconds. At pH = 2, the spectral features are the same, but the decay of the $^1Fl^*$ becomes faster. For example, the signal at 750 nm for pH = 3 solution decays up to ~80 % of its initial intensity by 1.2 ns, while the same signal for pH = 2 solution decays to ~60% of its initial intensity. Once the pH is lowered to 1.5, the difference becomes more readily observable. The decay of the signal at 750 nm occurs within several hundreds of picoseconds. In addition, an appearance of a new absorption band is obvious from the dynamics of the signal at 575 nm. The spectrum of this new transient can be inferred from the spectrum collected 1 ns after the excitation (lower right panel of Figure 5). It exhibits a broad and weak absorption in the 450–650 nm range.

This change in the excited state dynamics of FMN and FAD solutions is consistent with the excited state protonation of the isoalloxasine ring. Excited state proton transfer has been previously studied in a large number of organic compounds, usually photo-acids.[32–35] To prove the proton transfer mechanism, the authors usually performed H/D kinetic isotope effect measurement. In analogy, we compared the decay of FMN excited state at pH = 2 in H_2O and D_2O solutions. As we can see from Figure 6, the decay of FMN excited state in D_2O is slower than in H_2O, as expected for the rate constants of proton transfer reactions, with k_H/k_D ratio of 1.2. However, we compared the rates in D_2O and H_2O at other pH values, and we observed deuterium kinetic isotope effect at all pH values to a variable degree (data not shown). The deuterium effect at these pH values probably originates from the effect of N−H vibrational modes on the thermal deactivation of the FMN excited state. Thus, we cannot verify with certainty the proton transfer mechanism using deuterium isotope effect.

It was previously found that the acidity constant of the flavin derivatives in the excited state is $pK_a^* \sim 2.3$.[25] In our measurements, a large change in the dynamics occurs in the pH = 1.5–2 range, suggesting a somewhat lower value of the excited state acidity constant. We fitted the experimental data obtained at pH = 1.5 to a kinetic model presented in Scheme 3, according to which the initially produced flavin singlet excited state undergoes a protonation with the rate of $5.79 \times 10^9\ s^{-1}$. The spectrum of the protonated singlet excited state obtained from this fit is presented in the lower panel of Figure 7. For comparison, the upper panel of the Figure 7 presents the spectrum of $^1FlH^{+*}$ obtained by a direct excitation of FlH^+ (from the measurements of pH = −0.5 solution, see the previous section for more details). Interestingly, even though the two spectra show some similarity, they are not identical. In addition, the lifetime of $^1FlH^{+*}$ obtained by a direct excitation at pH = −0.5 is 280 ps, while the lifetime of $^1FlH^{+*}$ obtained by excited state protonation at pH = 1.5 is much longer, 470 ps. This result suggests that the protonation site of the isoalloxasine ring in the excited state is not the same as the protonation site that occurs with the molecule in the ground state. This is consistent with the calculations of the ground and excited state π-electron densities in flavins.[36] These calculations suggest that the protonation site of FMN in the ground state should be in the N1 position and in the N10 position for FMN in the excited state (Scheme 5).

FAD in the Neutral pH Range. While the FAD excited state behaves the same as FMN in the acidic (pH < 3) and basic (pH > 10) region, it exhibits different behavior in the neutral pH range. Figure 8 compares the dynamics of FAD and FMN solutions at pH = 7. As we can see from the decays obtained at 575 nm and 750 nm, the FMN excited state displays a long lifetime, on the order of several nanoseconds. On the other hand, the FAD excited state shows a short-lived component in its decay dynamics, with a lifetime of ~20 ps. The same results have already been reported by Stanley and MacFarlene.[16] The authors explain the observed fast deactivation dynamics of flavin ^1S state to be due to the stacking interaction between isoalloxazine and adenine moieties of FAD. On the basis of the reduction potential of flavin ($E_{red} = -0.3$ V)[37] and oxidation potential of adenine ($E_{ox} = 1.02$ V),[38] the mechanism of the

SCHEME 5: Representation of the protonation sites of FMN and FAD in the ground and excited states

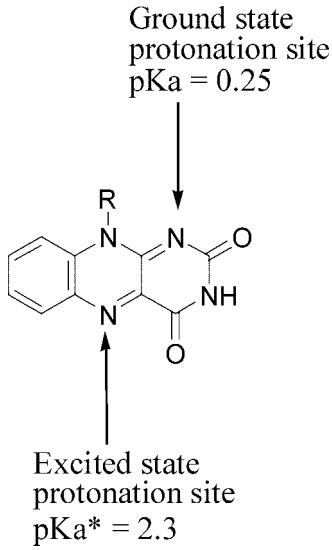

SCHEME 6: Schematic Representation of the Conformational Change in FAD Due to Adenine Protonation in the Acidic Region and Deprotonation in the Basic Region

SCHEME 7: Summary of FAD Excited State Behavior at Different pH Values

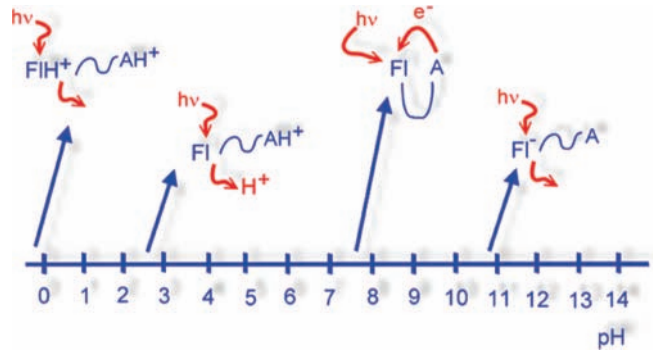

excited state deactivation could be a photoinduced electron transfer between these two moieties as shown in Scheme 7 (the free energy of the process should be $\Delta G = -1.3$ eV). However, we were not able to detect the signal arising from the radical ions produced in this process. The possible reason for this is that the charge separation and recombination processes are too fast to allow a detectable build-up of the radical ion concentration. This result is consistent with the previously published optical[16] and mid-IR[11] transient spectra of FAD.

An interesting point is that the rate of the FAD excited state deactivation does not change with the pH in the pH = 5–10 range. The pK_a value of the neutral flavin radical is pK_a = 8.3.[39] This value suggests that the electron transfer process should be accompanied by a proton transfer at pH < 8.3 to produce a neutral flavin radical, while only electron transfer should occur at pH > 8.3 to produce a flavin radical anion. The fact that we did not observe any difference in the rates of the excited state

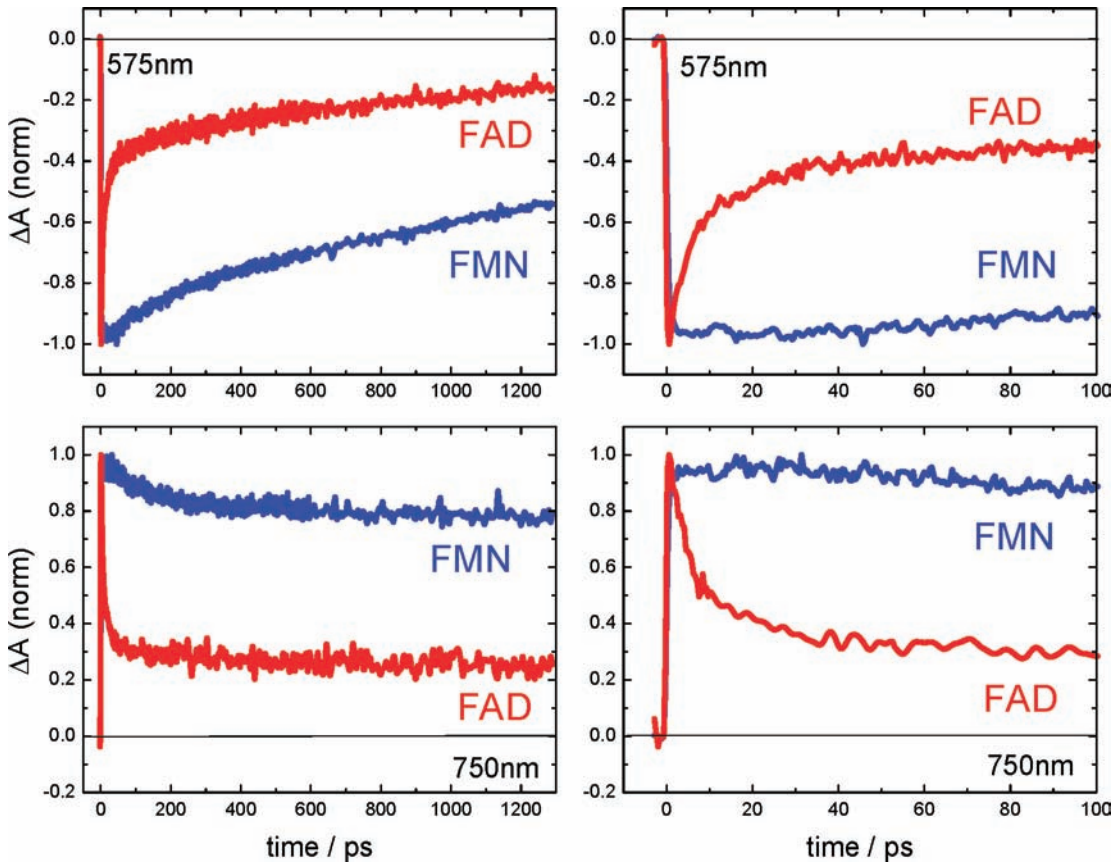

Figure 8. The decay dynamics of FMN (blue) and FAD (red) at 575 nm (upper panels) and 750 nm (lower panels). The measurements were done at pH = 7.

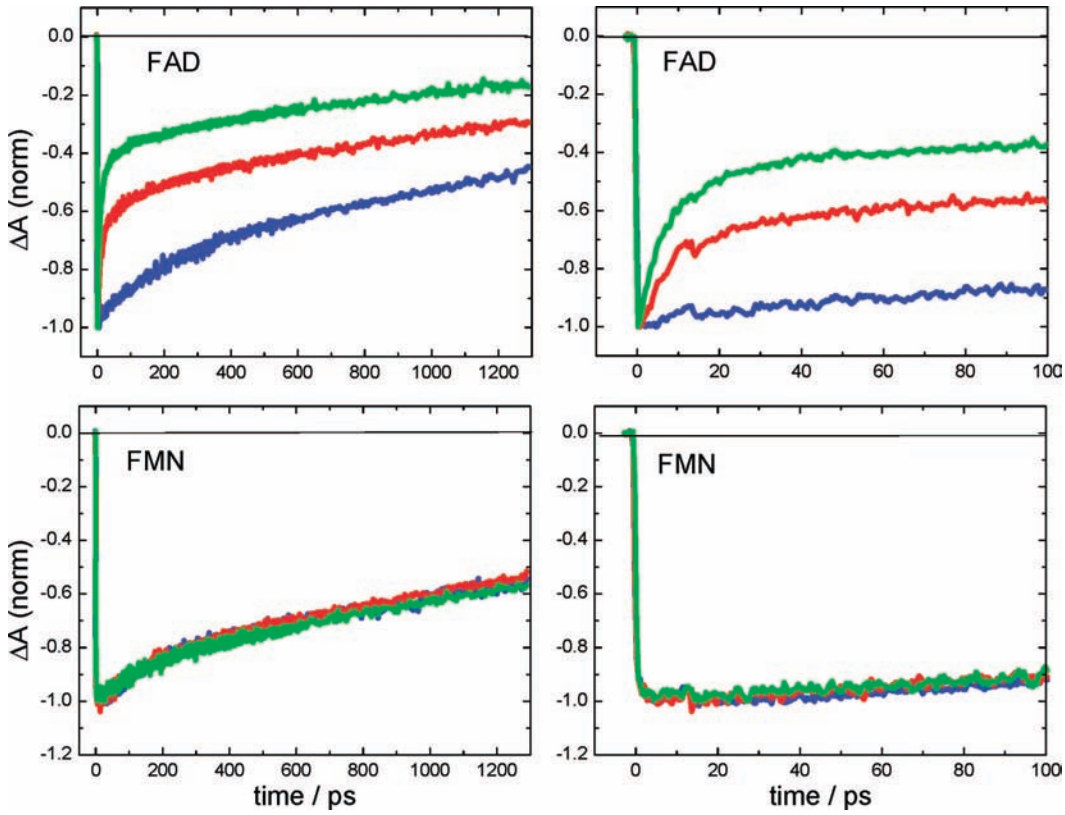

Figure 9. The decay dynamics for FAD (upper panels) and FMN (lower panels) at 575 nm. The solution pH values are as follows: pH = 3 (blue), pH = 4 (red), and pH = 5 (green).

deactivation suggests that the process does not occur via an electron transfer but rather via a fast thermal deactivation. However, the possibility that the rates of both processes are too fast to detect cannot be excluded.

Conformational Change in FAD. As the pH is lowered, FAD starts showing a steady increase in its excited state lifetime. This trend can be observed in Figure 9 which compares FAD and FMN excited state dynamics in the pH = 3–5 range. At pH = 5, FAD shows a fast decay component that arises because of the stacking interaction between isoalloxazine and adenine moieties of the molecule (see previous section). As the pH is lowered, the lifetime of the FAD excited state becomes longer and it becomes identical to FMN dynamics at pH = 3.

Since FMN does not exhibit this pH dependent behavior, the origin of the FAD dynamics in this pH range must arise because of the presence of the adenine moiety in the molecule. Since the pK_a value of the protonated adenine is 3.6,[40] we believe that the FAD undergoes a conformational change from "closed" to "open" form in this range because of the adenine protonation (Scheme 6). Another potential site of adenine protonation is its amino group. However, the pK_a value for the protonated adenine in its amino group position is estimated to be pK_a = −3,[41] so this process does not occur in the pH range we studied.

In the basic pH range, a similar conformational change can be observed. Figure 10 shows the excited state dynamics of FAD and FMN in the pH = 9–11 range. FMN shows an abrupt change in the dynamics at pH > 10.5, due to the ground state deprotonation of the N3 nitrogen on the isoalloxazine ring. The reported acidity constant for this process is pK_a = 9.75 (Scheme 2),[25] while it appears to be pK_a ∼ 10.75 from our measurements. This discrepancy is probably due to the different buffer solutions used. The change in the excited state dynamics observed in this pH range reflects the production of deprotonated FMN excited state, $^1Fl^-$*, which exhibits faster ISC rate relative to ^1Fl* (these rates were discussed in the previous section).

The excited state dynamics of FAD show a more complex behavior. At pH = 9.5, FAD exhibits a short lifetime due to the previously described stacking interaction between flavin and adenine moieties. As the pH is increased, FAD dynamics at 575 nm change and start to resemble those of the deprotonated FMN excited state. A large change in the FAD dynamics occurs at a lower pH than in the case of FMN, suggesting that FAD has a lower pK_a (∼10.25) value than FMN. The reason for this might be that the stacking between flavin and adenine moieties of FAD depletes the electronic density of the N−H bond of isoalloxazine ring, which leads to a more acidic molecule. At pH = 11, both FAD and FMN show identical dynamics, suggesting that FAD underwent a conformational change from "closed" to "open" conformation. Thus, the changes in the FAD excited state dynamics in this pH region reflect the conformational change induced by the deprotonation of the isoalloxazine ring (Scheme 6).

The exact structures of "open" and "closed" conformers are not known. However, some insight into their geometries has been obtained from the FAD conformations in various flavoproteins.[13] In most flavoproteins, FAD adopts an "open" conformation, which is stabilized by several hydrogen bonds in the sugar−phosphate backbone of the molecule. On the other side, the "closed" conformer is found in only few flavoproteins and is stabilized by the π-stacking interaction between the adenine and the isoalloxasine rings. Once the charge is introduced to one of these rings, either by protonation of the adenine moiety (pK_a = 3.6) or by deprotonation of the isoalloxazine ring (pK_a ∼ 10), the charged ring becomes hydrophilic and the solvation

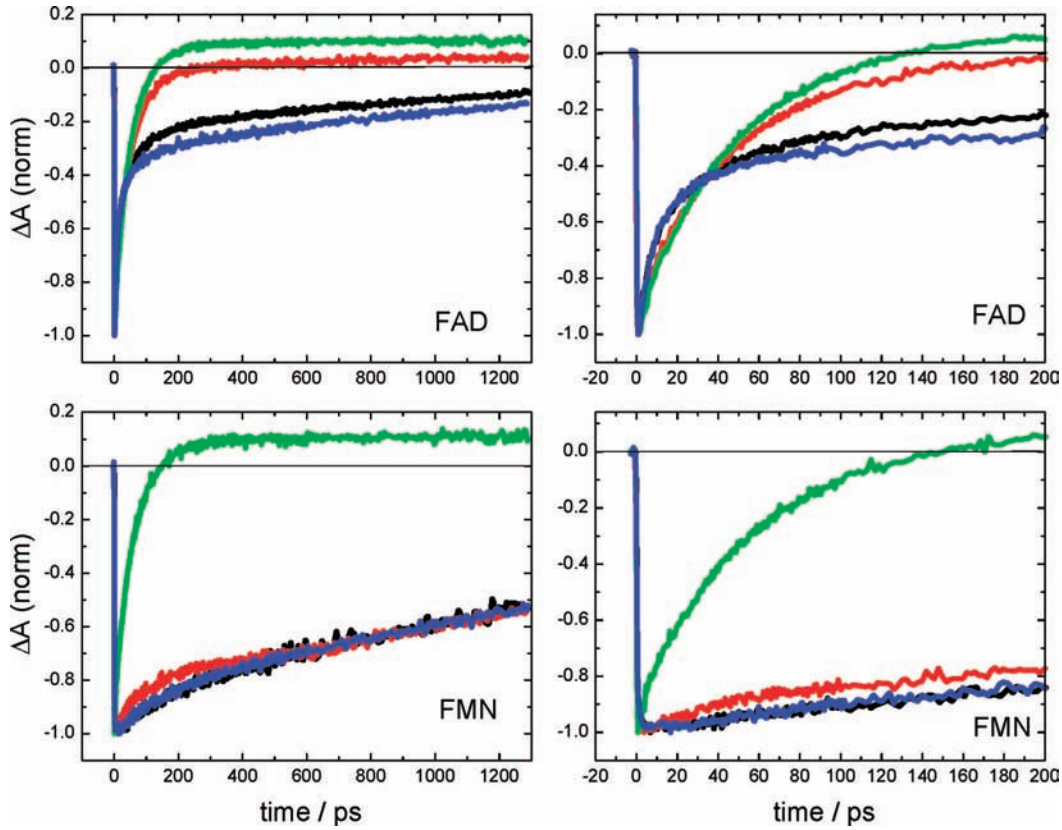

Figure 10. Transient absorption decays for FMN (upper panels) and FAD (lower panels) at 575 nm. The solutions pH values are as follows: pH = 9.5 (black), pH = 10 (blue), pH = 10.5 (red), pH = 11 (green).

of the charge induces breaking of the π complex and a conformational change to the "open" structure.

It is interesting to note that, in addition to the ground state deprotonation process, the lifetime shortening of flavins in this pH range might arise because of the deprotonation along the excited state potential energy surface. The excited state acidity can be easily estimated from the changes in the ground state absorption spectra upon deprotonation using a Forster cycle.[42] According to this method, a degree of wavelength shift in the absorption spectrum upon deprotonation reflects the acidity of the excited state:

Here, pK_a and pK_a^* are the ground and excited state acidity of the flavin, while $h\upsilon_{FlH}$ and $h\upsilon_{Fl^-}$ are the absorption energies of the protonated and deprotonated flavin. Using this cycle and the absorption spectra shown in Figure 1, we estimate the excited state acidity constant of flavin to be only 0.5 pH units smaller than the ground state acidity ($pK_a^* \sim 10.25$). Thus, the excited state deprotonation might occur in this pH range, but we are unable to resolve its dynamics from the ground state deprotonation process.

Conclusions

This article describes a study of pH dependence of the excited state dynamics of FAD and FMN using femtosecond optical transient absorption spectroscopy. The results are summarized in Scheme 7. We characterized the excited state absorption spectra for flavin in 3 states of protonation: Fl^-, Fl, and FlH^+. We find that Fl^- and Fl have similar excited state absorption spectra, but that the $^1Fl^{-*}$ intersystem crossing rate is much higher than that of Fl*. The transient absorption spectrum of FlH^{+*} is significantly different from other forms, suggesting a high degree of electronic redistribution in the chromophore upon protonation. We further investigated the excited state protonation of flavin and found that the molecules in the ground and excited states exhibit different protonation sites. In the case of FAD, we find that its excited state dynamics are controlled by the level of stacking between isoalloxazine and adenine rings. At low and high pH values, FAD adopts an "open" conformation, and its excited state dynamics are identical to those of FMN. The conformational change occurs because of the protonation of the adenine ring at low pH and deprotonation of the isoalloxazine ring at high pH. In the neutral pH range, FAD adopts a "closed" conformation and exhibits a fast excited state deactivation due to the stacking interaction between the two aromatic moieties.

We are currently investigating the same flavin systems using mid-IR transient absorption spectroscopy with hope that our results will provide valuable information for the future analysis of flavoproteins using pump−probe spectroscopy.

Acknowledgment. The research reported is supported by PRF (Grant 46807-G4) and by start-up funds from Bowling Green State University. We thank Michael J. Rodgers and Eugene Danilov for their help with the laser measurements.

References and Notes

(1) Vangrondelle, R.; Dekker, J. P.; Gillbro, T.; Sundstrom, V. *Biochim. Biophys. Acta* **1994**, *1187*, 1–65.
(2) Birge, R. R. *Biochim. Biophys. Acta* **1990**, *1016*, 293–327.
(3) Cashmore, A. R.; Jarillo, J. A.; Wu, Y. J.; Liu, D. M. *Science* **1999**, *284*, 760–765.
(4) Sancar, A. *Ann. Rev. Biochem.* **2000**, *69*, 31–67.
(5) Sancar, A. *Chem. Rev.* **2003**, *103*, 2203–2237.
(6) Briggs, W. R.; Christie, J. M. *Trends Pl. Sci.* **2002**, *7*, 204–210.
(7) Gomelsky, M.; Klug, G. *Trends Biochem. Sci.* **2002**, *27*, 497–500.
(8) Cashmore, A. R. *Cell* **2003**, *114*, 537–543.

(9) Barrio, J. R.; Tolman, G. L.; Leonard, N. J.; Spencer, R. D.; Weber, G. *Proc. Nat. Acad. Sci.* **1973**, *70*, 941–943.
(10) Heelis, P. F. *Chem. Soc. Rev.* **1982**, *11*, 15–39.
(11) Kondo, M.; Nappa, J.; Ronayne, K. L.; Stelling, A. L.; Tonge, P. J.; Meech, S. R. *J. Phys. Chem. B* **2006**, *110*, 20107–20110.
(12) Grininger, M.; Seiler, F.; Zeth, K.; Oesterhelt, D. *J. Mol. Biol.* **2006**, *364*, 561–566.
(13) van den Berg, P. A. W.; Feenstra, K. A.; Mark, A. E.; Berendsen, H. J. C.; Visser, A. *J. Phys. Chem. B* **2002**, *106*, 8858–8869.
(14) Chosrowjan, H.; Taniguchi, S.; Mataga, N.; Tanaka, F.; Visser, A. *Chem. Phys. Lett.* **2003**, *378*, 354–358.
(15) Copeland, R. A.; Spiro, T. G. *J. Phys. Chem.* **1986**, *90*, 6648–6654.
(16) Stanley, R. J.; MacFarlane, A. W. *J. Phys. Chem. A* **2000**, *104*, 6899–6906.
(17) Raszka, M.; Kaplan, N. O. *Proc. Nat. Acad. Sci.* **1974**, *71*, 4546–4550.
(18) Stob, S.; Kemmink, J.; Kaptein, R. *J. Am. Chem. Soc.* **1989**, *111*, 7036–7042.
(19) Islam, S. D. M.; Susdorf, T.; Penzkofer, A.; Hegemann, P. *Chem. Phys.* **2003**, *295*, 137–149.
(20) Murakami, M.; Maeda, K.; Arai, T. *J. Phys. Chem. A* **2005**, *109*, 5793–5800.
(21) Nikolaitchik, A. V.; Korth, O.; Rodgers, M. A. J. *J. Phys. Chem. A* **1999**, *103*, 7587–7596.
(22) Ford, W. E.; Rodgers, M. A. J. *J. Phys. Chem.* **1994**, *98*, 3822–3831.
(23) Yamaguchi, S.; Hamaguchi, H. O. *App. Spect.* **1995**, *49*, 1513–1515.
(24) Gampp, H.; Maeder, M.; Meyer, C. J.; Zuberbuhler, A. D. *Talanta* **1985**, *32*, 95–101.
(25) Drossler, P.; Holzer, W.; Penzkofer, A.; Hegemann, P. *Chem. Phys.* **2002**, *282*, 429–439.
(26) Song, P. S.; Metzler, D. E. *Photochem. Photobiol* **1967**, *6*, 691.
(27) Moore, W. M.; Spence, J. T.; Raymond, F. A.; Colson, S. D. *J. Am. Chem. Soc.* **1963**, *85*, 3367–3372.
(28) Song, S. H.; Dick, B.; Penzkofer, A. *Chem. Phys.* **2007**, *332*, 55–65.
(29) Murakami, M.; Maeda, K.; Arai, T. *Chem. Phys. Lett.* **2002**, *362*, 123–129.
(30) Climent, T.; Gonzalez-Luque, R.; Merchan, M.; Serrano-Andres, L. *J. Phys. Chem. A* **2006**, *110*, 13584–13590.
(31) Siebrand, W. *J. Chem. Phys.* **1967**, *47*, 2411–2422.
(32) Arnaut, L. G.; Formosinho, S. J. *J. Photochem. Photobiol.* **1993**, *75*, 1–20.
(33) Formosinho, S. J.; Arnaut, L. G. *J. Photochem. Photobiol.* **1993**, *75*, 21–48.
(34) Solntsev, K. M.; Clower, C. E.; Tolbert, L. M.; Huppert, D. *J. Am. Chem. Soc.* **2005**, *127*, 8534–8544.
(35) Spry, D. B.; Goun, A.; Glusac, K.; Moilanen, D. E.; Fayer, M. D. *J. Am. Chem. Soc.* **2007**, *129*, 8122–8130.
(36) Song, P.-S. *Photochem. Photobiol.* **1968**, *7*, 311.
(37) Braun, R. B. *J. Electrochem. Soc.* **1977**, *124*, 1342.
(38) Goyal, R. N.; Oyama, M.; Singh, S. P. *Electroanalysis* **2007**, *19*, 575–581.
(39) E. J. Land, A. J. S. *Biochem. Adv. Phys. Org. Chem.* **1969**, *8*, 2117.
(40) Saenger, W. *Principles of Nucleic Acid Structure*; Springer: New York, 1988.
(41) McGhee, J. D.; Von Hippel, P. H. *Biochem.* **1975**, *14*, 1281–1296.
(42) J. F. Ireland, P. A. H. W. *Adv. Phys. Org. Chem.* **1976**, *12*, 131.

JP7117218